AIAA JOURNAL
Vol. 45, No. 2, February 2007

Probabilistic Modeling of Aerothermal and Thermal Protection Material Response Uncertainties

Michael J. Wright,* Deepak Bose,† and Y.-K. Chen‡
NASA Ames Research Center, Moffett Field, California 94035

DOI: 10.2514/1.26018

A Monte-Carlo-based methodology is presented for physics-based probabilistic uncertainty analysis of aerothermodynamics and thermal protection system (TPS) material response modeling for aerocapture or direct entry missions. The objective of the methodology is to identify and quantify the most important sources of uncertainty in aeroheating and the resulting thermal protection material selection, design, and sizing based on inaccuracies in current knowledge of the parametric input modeling parameters. The resulting parametric modeling uncertainty would be combined with other uncertainty sources to determine the final aeroheating and TPS response modeling uncertainty for a given application, which can then be used to define appropriate margins and factors of safety that should be applied to the TPS. These techniques facilitate a risk-based probabilistic design approach, whereby the thermal protection system can be designed to a desired risk tolerance, and any remaining risk can be effectively compared to that of other subsystems via a system-level risk mitigation analysis. Modeling sensitivities, which are a byproduct of the uncertainty analysis, can be used to rank input uncertainty drivers. Key input uncertainties can then be prioritized and targeted for further analysis or testing. The strengths and limitations of this technique are discussed. Sample results are presented for two cases: Titan aerocapture and Mars Pathfinder. These cases demonstrate the utility of the methodology to quantify the uncertainty levels, rank sources of input uncertainty, and assist in the identification of structural uncertainties in the models employed.

I. Introduction

ANY Earth or planetary entry vehicle will be subjected to significant aerothermal heating as it dissipates its kinetic energy at the destination planet (or moon). The same is true for aerocapture, a technology in which an aeroshell is used to dissipate kinetic energy at the destination planet via atmospheric drag instead of an onboard propulsion system [1]. In each application, the primary purpose of the thermal protection system (TPS) is to protect the payload (crew or science) from this entry-heating environment. The performance of the TPS is therefore determined by the efficiency and reliability of this system throughout all anticipated operating environments. A typical system performance metric is the mass of thermal protection material and support structure required to ensure the safety of the payload to a prescribed level of risk tolerance. This performance metric is particularly important for an aerocapture mission, for which the ultimate decision to select this technology for a given mission is determined in part by the propellant and propulsion system mass savings as compared to the mass of the vehicle TPS required to protect the payload from the entry heating [2].

Therefore, for any rigid aeroshell, the material selection and design (margined) thickness of the selected TPS material define two of the key performance metrics of the entire entry system. The choice of the TPS material is typically governed by the peak heat flux, surface pressure, and shear stress encountered during the entry, with more robust (higher density) materials required to protect the vehicle from more severe entry conditions. Once a material has been selected, the design thickness is governed primarily by the total integrated heat load during the entry (which can be very large for aerocapture or high-lift entry missions, due to a long residence time in the atmosphere). The accurate determination of each of these quantities relies on high-fidelity aerothermodynamics and material response modeling, including estimated uncertainties in the predicted values.

Although in current design practice baseline predictions are made using high-fidelity modeling and simulation tools, the evaluation of their associated uncertainties often involves comparatively little or no rigorous analysis. However, an accurate determination of these uncertainties is critical in determining the safety margin on material thickness, a significant contributor to the overall mass of the TPS. Artificially large uncertainties on aeroheating predictions could unnecessarily limit the available material choices, forcing the selection of a more robust (i.e., heavier) material than is actually required. This cascading conservatism can also reduce or eliminate the apparent advantage of aerocapture over traditional propulsive deceleration for a given mission. More important, without a rigorous estimate of the design uncertainties employed, an accurate assessment of the TPS subsystem risk cannot be performed. For some missions of interest, minimizing TPS mass is of secondary importance (for example, a heavier TPS can make it easier to separate the aeroshell from the payload, or can move the center of gravity forward to increase vehicle stability). However, TPS risk and reliability are always primary concerns. An accurate assessment of TPS risk is required to ensure that the TPS design is consistent with the risk posture of the program, and can be incorporated with probabilistic risk assessment and probabilistic design techniques [3,4] so that engineers can make informed decisions on ways to effectively balance mission risk between the TPS and other vehicle subsystems.

Historical approaches for dealing with these uncertainties have traditionally been somewhat ad-hoc, relying on expert judgment to assign uncertainty levels to the various elements of the aeroheating predictions and TPS sizing estimates [5]. Even when rigorous attempts at uncertainty estimation were attempted [6–8], computational resource limitations prevented the sort of nonlinear multivariate analysis that is truly required. Once uncertainty components have been identified, final "rolled-up" uncertainties are then typically determined using either a stacked worst-case approach, which can be needlessly conservative, or a root-sum-square approach [9], which is only appropriate for a set of small

Received 20 June 2006; revision received 10 October 2006; accepted for publication 12 October 2006.

*Senior Research Scientist, Reacting Flow Environments Branch, MS 230-2. Senior Member AIAA
†Senior Research Scientist, ELORET Corporation. Member AIAA
‡Senior Research Scientist, Thermal Protection Materials and Systems Branch, MS 234-1. Senior Member AIAA

linearly independent errors. Worse yet, either of these approaches may in fact be nonconservative if the underlying component uncertainties are not estimated correctly [6]. Although we believe that a planetary entry capsule TPS has never failed during entry, this finding should be considered more a testament to the inherent conservatism of design engineers than a validation of the uncertainty analysis approaches applied. However, as NASA missions become larger and more ambitious it will become increasingly difficult to bury uncertainties under large design margins. Requirements for future crewed entry systems, such as the Crew Exploration Vehicle (CEV), will be even more rigorous, necessitating accurate knowledge of inherent uncertainties and resulting risks to satisfy human-rating requirements and ensure crew safety during entry. In addition, a new class of ambitious crewed and robotic entries will require extrapolation of existing models to new untested conditions, which could result in unanticipated failures if a more rigorous design approach is not adopted. The Galileo entry probe to Jupiter, which entered on 7 December 1995, is a prime example. Whereas this mission was successful, postflight analysis of the heat-shield engineering data obtained during the entry revealed that TPS recession on the shoulder was much greater than predicted, nearly leading to a burn-through [10]. Although the specific reasons for this anomaly are still not known, the fact that the predictions did not agree with the observed performance implies that there were inadequacies in the physical models employed in the TPS design for this extreme environment.

This paper will present a methodology for physics-based probabilistic uncertainty analysis of aerothermodynamics and material response modeling. A primary objective is to quantify the uncertainties in vehicle heating and the resulting TPS sizing based on inaccuracies in the knowledge of the input parameters, such as reaction rates, relaxation rates, surface catalysis, and material and transport properties. In addition to quantifying the uncertainty in the aeroheating and TPS sizing predictions, the technique will allow us to isolate the chief sources of input uncertainty in the models. These uncertainty drivers can then be prioritized and targeted for further ground-based testing [11] or possible flight instrumentation to maximize the return from limited research funding. A sensitivity analysis, which is a byproduct of the full uncertainty analysis, also provides valuable insights by identifying rate-limiting steps, discontinuous transitions (such as reaching a material spallation limit), and the trends of the dominant mechanisms in the physical model. The results of the sensitivity analysis can also be used to identify possible additional uncertainties due to erroneous or overly simplified physical models (also known as structural uncertainties); if the models employed are correct, the sensitivities predicted by the analysis should be reproducible via targeted experiments. Identification of structural uncertainties is a key element of this work, because a large undetected structural uncertainty can invalidate the remainder of the uncertainty results. An example of using this analysis to aid in the identification of a potential structural uncertainty will be given in the results section. Finally, the results of the analyses described herein are a valuable tool that can be used in the design of ground-based experiments and flight data acquisition. Once this analysis is complete, the designer is better equipped to justify and focus experimental efforts. Uncertainties that are determined to already be below the design requirements (or detectability threshold) can be lowered in priority and the engineer can concentrate on designing tests and selecting instrumentation types and locations that will best inform key remaining uncertainties in the models employed.

In this work a Monte Carlo technique will be presented and used to statistically track the propagation of various input uncertainties into the uncertainty of the vehicle heating predictions made by a reacting gas thermochemical nonequilibrium computational fluid dynamics (CFD) code and an ablating TPS material response code. A fully nonlinear analysis (rather than a simple linear approach) is necessary because the input uncertainties are large and the physical models are inherently nonlinear. The strengths and limitations of this technique are discussed. Sample uncertainty analysis results are presented for a proposed Titan aerocapture mission and the Mars Pathfinder entry vehicle. These cases demonstrate the utility of the methodology to quantify the uncertainty levels in aeroheating and TPS sizing predictions, rank sources of input uncertainty for further targeted analysis, and facilitate identification of structural uncertainties in the models employed. Additional examples of Monte-Carlo-based TPS analyses are given in [12].

It is important to note that a Monte Carlo nonlinear uncertainty analysis requires hundreds or thousands of individual CFD and/or material response calculations to build meaningful statistics. Until recently, such a task would have been beyond the capabilities of existing codes and computational resources. However, recent advances in parallel computers (particularly inexpensive workstation clusters), as well as new parallel algorithms that have been designed for efficiency in such an environment, have made these analyses possible. A typical axisymmetric nonequilibrium reacting flow CFD calculation such as described in the Results section can now be performed in less than a minute on eight CPUs of a commodity workstation cluster, meaning that a full uncertainty analysis of 3000–6000 CFD runs can be carried out in about two–four days on such a machine. Full three-dimensional analyses would require several weeks of computation, but are still possible if a suitable axisymmetric analog of the desired analysis is not available.

II. Types of Input Uncertainty

The design aerothermodynamic environment of a planetary entry or aerocapture vehicle is typically predicted via high-fidelity thermochemical nonequilibrium CFD codes such as DPLR [13] at NASA Ames and LAURA [14] at NASA Langley. The thermochemical response, including pyrolysis and ablation, of the TPS material is simulated with a material response code such as CMA [15] or FIAT [16]. Over the years these codes have been calibrated against each other and validated with a variety of experimental data from ground and flight tests [17–21]. Based on these analyses, it can be clearly demonstrated that the predictions made by these tools are highly sensitive to the physical, chemical, and (to a lesser extent) numerical models employed, as well as the multitude of parameters that these models introduce [5]. As a result, the net uncertainty in the heating and TPS sizing predictions is a result of a combined effect of the uncertainties in all of the models and input parameters used in the analysis. Therefore, to place confidence levels on an aeroheating or TPS sizing calculation, all of the chief sources of input uncertainty must be identified and quantified. The propagation of these uncertainties through the chosen model must then be tracked to make probabilistic estimates of the resulting quantities, in the form of a most probable result and a probability distribution characterizing the variability of the prediction.

The primary sources of uncertainty in the thermochemical models used in aerothermal and TPS analysis, like other physical models, can be classified into three major categories: stochastic variability, structural uncertainty, and parametric uncertainty. Each of these is discussed in detail in the following subsections.

A. Stochastic Variability

This type of uncertainty arises due to natural fluctuations that exist in the physical environment. It is also known as irreducible uncertainty, meaning that it can be characterized, but not reduced, through experimentation and analysis. Examples in TPS design include natural fluctuations in atmospheric conditions and thermal protection material surface texture variations arising from long-duration space exposure. This type of uncertainty is routinely modeled in 3 degree-of-freedom (DOF) or 6-DOF entry trajectory simulations using a Monte Carlo approach [22]. Stochastic uncertainties can easily be modeled in the analysis procedure outlined herein, provided that the input variabilities can be quantified and parameterized.

B. Structural Uncertainty

All numerical simulation methods employ a mathematical model of the physics, such as the reacting Navier–Stokes equations for

hypersonic fluid flow. The model employed is invariably an approximation of reality that uses a set of simplifying assumptions to represent the physical phenomena being studied. These simplifications, mostly incorporated for the purposes of tractability, are valid over only a limited range of conditions, and as such can be a significant source of uncertainty. Examples of these uncertainties in thermochemical models include such things as the limitations inherent in the continuum form of the governing equations, representation of their boundary conditions, assumption of a specific (e.g., equilibrium) energy distribution function, geometric simplifications, and perhaps the impact of previously unknown physical mechanisms. Furthermore, the mathematical equations employed must be discretized to be put in a form that is amenable to numerical simulation. This further simplification can lead to discretization or truncation errors in the final computational model. Put simply, structural uncertainties arise when either the physical model employed or its numerical discretization is incorrect or insufficient to describe the phenomenon under study. For example, using the incompressible Navier–Stokes equations for a hypersonic flow, or neglecting shock-layer radiation effects for estimates of Apollo capsule reentry heating would be examples of structural uncertainties. More commonly, simplified physical models (such as the Wilke mixing rule [23] for mixture viscosity) are, mistakenly or intentionally, used for simulations at conditions outside of those for which the models were developed or intended. Obviously the potential for structural uncertainties is larger in regimes for which the models employed have not been properly validated.

C. Parametric Uncertainty

This type arises from the uncertainties in the input model parameter estimates. A typical TPS sizing calculation can include hundreds of these input parameters, such as chemical reaction rates, energy relaxation rates, vibration–dissociation coupling parameters, laminar and turbulent transport properties, turbulent transition criteria, surface catalycity and emissivity, TPS recession rates, virgin and char material properties, shock-layer radiation emission and absorption rates, and others. Whereas a large number of these parameters are required for such computations, only a small subset of them have been experimentally measured or theoretically calculated at conditions relevant for planetary reentry vehicles. A large majority of the required parameters are therefore estimated either by indirect or purely empirical techniques. Even for those input parameters that have been measured or calculated at relevant conditions, uncertainties remain due to limitations of the experimental or theoretical methods employed, extrapolation to flight conditions, or other reasons. Parametric uncertainties can generally be reduced, but not eliminated, via focused testing or analysis.

III. Quantification of Structural Uncertainty

The current paper focuses on a methodology to quantify and track the propagation of parametric uncertainties that arise in a given physical model. Stochastic variabilities will not be considered, although it should be noted that the effects of stochastic variability can be readily coupled to parametric uncertainties in a high-fidelity analysis, for example, by coupling a 6-DOF trajectory code to a CFD and material response package. This type of coupled probabilistic/stochastic analysis was first presented by Dec and Mitcheltree for a proposed Mars Sample Return mission [24]. In contrast, structural uncertainties cannot be quantified or even directly identified by Monte-Carlo-based analysis alone. In fact, a significant structural uncertainty in the model employed can completely invalidate the results of a Monte-Carlo-based analysis, because the predicted trends and correlations that result will be those of the chosen model, not necessarily reality. One of the assumptions of this analysis is that all significant structural uncertainties have been independently identified and quantified (or eliminated) before the parametric analysis. However, the analysis approach presented here can be used to assist in the design of experiments that will expose structural uncertainties by displaying trends that are inconsistent with those predicted. In particular, the analysis presented here can be employed to predict the nonlinear behavior of the system with respect to experimentally controllable quantities (such as temperature, pressure, gas composition, etc.). The resulting sensitivities can then be tested experimentally to ensure that the model is predicting the correct trends.

As discussed in the preceding section, structural uncertainties can in general be divided into two types: uncertainty due to numerical discretization errors, and uncertainty due to inadequate physical models. Whereas it is beyond the scope to discuss the identification and elimination of these structural uncertainties in detail, a brief review is provided here.

Structural uncertainties due to numerical discretization errors are best handled via rigorous code verification, as discussed by Roache [25] and Roy et al. [26]. According to AIAA [27], code verification is the process of determining that a model implementation accurately represents the developer's intentions. In other words, is the model employed correctly implemented? Several techniques are commonly employed in code verification, including the method of manufactured solutions [28], by which nontrivial exact solutions of the governing equations are constructed and used to verify the accuracy of the discretized form. Roy et al. [26] provides a good overview of the types of methodologies employed for code verification purposes. In general, some verification of the code employed and its various numerical methodologies should be performed as part of the software acceptance or quality control process before its application to actual TPS design [29]. In addition, application-specific code verification studies (e.g., grid alignment and resolution) should be performed for the particular design problem of interest before application of the uncertainty methodology discussed in this paper.

On the other hand, structural uncertainties due to inadequate or improper physical models are best addressed by code validation [25,30]. Again, according to AIAA [27], code validation is the process of determining the degree to which a given model is an accurate representation of the real world. In other words, does the model employed include the correct physics to model the phenomenon under study? Code validation is most commonly accomplished by comparison of computational predictions to the results of targeted ground or flight testing. This approach poses significant challenges in the field of TPS design, because flight data are typically extremely scarce, and generally no ground facility can simultaneously reproduce all important aspects of the flight environment. Therefore, it is crucial that ground tests are carefully designed, and that traceability of ground test results to the flight environment be maintained [31].

One final potential source of structural uncertainty is that due to poor process [29]. A fully validated and verified code can still produce incorrect results if used incorrectly [32]. One of the dangers of modern computational tools is that it is easy to believe that whenever the code produces a "converged" answer, it is an accurate result. The best way to avoid this trap is to ensure that discipline experts are involved in every step of the analysis process. The definition of and adherence to a well-formulated CFD process should be an important part of any aerothermal/TPS design; however, the specifics of such a process are beyond the scope of the current work.

IV. Sensitivity and Uncertainty Analysis

A. Local Analysis

For linear systems and/or systems where the uncertainties at play are small, a linear analysis may be used. In such an analysis, sensitivity coefficients $\partial y_i/\partial x_j$ that determine the change in the output parameter y_i caused by an infinitesimal change in the input parameter x_i from its reference or most probable value are evaluated. The sensitivity coefficients can be computed numerically by recording the changes in the output as each input parameter is varied by an infinitesimal amount while all other parameters are held constant. Alternatively, sensitivity coefficients may be obtained by differentiating the governing equations with respect to all input parameters and solving the resulting system of equations with the desired sensitivity coefficients as the unknowns. This approach is

known as an adjoint model. In any case, once the coefficients are determined, the uncertainty in the output parameter is described by the law of propagation of errors:

$$\sigma^2(y_i) = \sum_k \left(\frac{\partial y_i}{\partial x_k}\right)^2 \sigma^2(x_k) \tag{1}$$

where $\sigma^2(y_i)$ is the variance (uncertainty) in the value of the output parameter y_i, and $\sigma^2(x_k)$ is the corresponding variance in the input parameter x_k. The input parameter (e.g., reaction rate, transport coefficient, etc.) uncertainties are determined either from the original literature sources or via expert judgment. Methods for determining input uncertainty will be discussed in a later section. Although computationally efficient, the linear analysis outlined here is purely local in nature, i.e., the analysis yields sensitivity coefficients only in the neighborhood of the baseline values in parameter space. However, in practice the variability in input parameters can be quite large in aerothermal and material response analysis. The sensitivity coefficients may not only vary substantially within the parameter space, but may also interfere with the sensitivities of other input parameters due to nonlinearities in the underlying physical models. Therefore, a nonlinear global uncertainty analysis is necessary.

B. Global Analysis

Apart from the ability to treat nonlinearities and large variabilities in the input and output parameters, a global model allows simultaneous variation of input parameters to account for uncertainty and sensitivity interference effects. Although there are many possible statistical approaches available for the analysis of nonlinear systems, we have chosen the Monte Carlo technique, which relies on probability-sampling techniques to determine sensitivities and uncertainties in the numerical model under study. Whereas Monte Carlo analysis converges slower than other methods (the convergence rate is proportional to the square root of the number of samples), it has the advantage that the rate of convergence is independent of the number of input variables considered [4]. This feature makes the Monte Carlo approach attractive for this type of aerothermal/TPS sizing analysis, where there can be literally hundreds of independent input modeling parameters in a given simulation.

In the Monte Carlo technique, the entire set of input parameters is varied independently using probability distribution functions. Except where otherwise noted, we choose a Gaussian function to describe the uncertainty of each input parameter; the maximum of the function is set at the recommended value, and the width of the curve represents the uncertainty (variability) in the parameter. We assume that the probability distribution functions are symmetric about the recommended value. It is also assumed that the uncertainties of the input parameters are uncorrelated. Input correlations occur when the set of input parameters chosen for the analysis are not linearly independent from each other; that is, a trend towards positive or negative uncertainty in one input parameter directly affects sign or magnitude of the uncertainty of another input. It is important to note, however, that these assumptions are not explicitly imposed by the selected Monte Carlo technique; rather, they are necessitated by a lack of detailed information on the myriad of input uncertainties. Non-Gaussian distribution functions can be easily incorporated into the present technique if sufficient data are available to model these effects. Relationships (correlations) between input parameters can also readily be modeled in the analysis if the functional forms of the relationships are known a priori (which is seldom the case). Input correlations can also be detected using principal component analysis (PCA), by which a large set of correlated input variables can be transformed into a smaller set of uncorrelated variables by means of eigenvalue analysis of their correlation matrix [33]. This process is mathematically equivalent to deriving a set of linearly independent eigenvectors in linear algebra.

It is beyond the scope of the current paper to fully describe the details of the Monte Carlo analysis technique, but the major steps in the process (as tailored for TPS analysis) are briefly outlined here. For a full description of the statistical methods employed see [34].

1) Problem Definition: The first step is to clearly and succinctly identify the purpose of the analysis and to ensure that the chosen simulation tool(s) have been validated for the given analysis. This step, which is overlooked surprisingly often, includes an accurate and succinct definition of the problem statement, states the objectives of the sensitivity study, and clearly identifies the set of physical models that should be employed in the analysis.

2) Parameter Identification: Input variables that need to be varied are first identified. Input variables include all modeling parameters required by the physical and numerical models employed in the simulation. In an aerothermal CFD code, input variables include such things as reaction rate parameters, vibration–dissociation coupling parameters, vibrational–translational relaxation times, binary interaction collision integrals for transport property calculations (diffusion, viscosity, and thermal conductivity coefficients), wall catalycity parameters, and possibly even freestream conditions. In a TPS material response code the variables include virgin and char thermal conductivity, specific heats, surface emissivity, recession rates, initial cold soak temperature, and properties of the underlying substructure. For a full analysis of an ablating TPS there are often hundreds of input modeling parameters, typically taken from the literature [35–37]. Note that not all input variables in a given simulation are necessarily varied in each uncertainty analysis; the choice of quantities to vary is dependent on the outcome desired (the problem definition determined in the preceding step). For example, if it is desired to examine only the impact of numerics on the output uncertainty, physical modeling parameters may be held constant while numerical algorithm parameters are varied.

3) Initial Uncertainty Estimation: Variability limits for all selected input parameters are chosen that roughly represent their typical uncertainties. The chosen variability limits need not represent the true estimated input uncertainties at this point, because they will only be used for an initial sensitivity analysis. However, it is important that they are conservative; underestimating an uncertainty for a given parameter will lessen its correlation in the resulting sensitivity analysis. The penalty for overestimating the magnitude of certain input uncertainties at this point is (at worst) an increase in the number of input parameters for which accurate uncertainties must be determined in step 6. On the other hand, if one or more input uncertainties are severely underestimated, they may be erroneously neglected as significant contributors to the overall output uncertainty.

4) Sensitivity Analysis: A global sensitivity analysis is then performed by randomly varying each of the input parameters to generate input files that are then used to run CFD and/or material response simulations to obtain corresponding heat fluxes and TPS sizing estimates. Each input parameter is independently and simultaneously varied about its baseline value using an appropriate probability distribution function. A symmetric Gaussian distribution is commonly employed for this purpose; however, other symmetric or asymmetric distributions are possible, as stated earlier. At this point any known correlations between input parameters can be accounted for via logic in the code that generates the input variable sets for each case. It is important that sufficient runs are made for each case to ensure statistical accuracy of the resulting sensitivities. Typically hundreds to thousands of runs are required, depending on the desired accuracy of the output data.

5) Correlation Coefficient Computation: Input–output correlation coefficients are computed using regression analysis and the fractional contribution of each input variability to the overall output variability is obtained. The largest contributors are then simply identified as those that cause the most sensitivity to predicted output (e.g., heat flux or material thickness). For most cases the majority of the correlation is due to a small number of input parameters; the vast majority display minimal sensitivity, and thus warrant no further analysis. This step allows us to shortlist a small subset of the parameters for a more detailed investigation. Note that at the current time only direct (single parameter) correlations are computed.

Multiparameter correlations (interference effects) could also be computed at this stage to increase the fidelity of the sensitivity results.

6) Final Input Uncertainty Estimation: A more accurate estimate of the associated uncertainties for the reduced list of input parameters is then made. This step can be one of the most time-consuming parts of the entire process, which is why a detailed assessment is deferred until the input uncertainties have been shortlisted via a sensitivity analysis. Clearly the fidelity of the final results depends strongly on the accuracy of the uncertainties assigned to the most sensitive input parameters. Additional information on the methods employed to determine quantified input uncertainties is given in Sec. V.

7) Uncertainty Analysis: A second set of CFD and/or material response calculations is then made. For this run the variabilities of the shortlisted parameters are adjusted according to their estimated uncertainties from the preceding step, whereas all other parameters are varied according to the initial estimates. It is necessary to vary all input parameters in this step, even those that were not identified by the sensitivity analysis, for two reasons. First, even though each individual input parameter may not contribute much to the final uncertainty, the cumulative effect of all of them can be significant. Second, although some parameters may not show up with large sensitivity in the linear correlation analysis, their effects may be important through interference effects. The full analysis will capture the uncertainty due to interference effects even if they were not identified explicitly, as long as the parameters are allowed to vary. The function of this step is to create a database of simulation data that can be statistically analyzed. It is important to note that this database consists of full multidimensional CFD and/or material response data, which can be a valuable future resource. Although the intent of a given study may be narrowly focused (e.g., stagnation point heating rate), the database contains much more information (such as shock standoff distance, peak shock temperature, shear stress, etc.), which can be analyzed at a future time with minimal cost.

8) Apportionment of Output Uncertainty into Input Parameters: At the completion of step 6, the variability in the output quantity of interest represents the true parametric uncertainty of the model to the desired level of fidelity. Finally, input–output correlations are again computed and ranked to apportion the output uncertainty into those of input parameters.

Note that, for a nonlinear system, it is generally not possible to rigorously separate the contributions of each input parameter to the output uncertainty. Nevertheless, a linear regression analysis is often employed to roughly gauge the uncertainty contributions. In this analysis, the square of the correlation coefficient, r_{ij}^2, is given by

$$r_{ij}^2 = \left(\sum_k (x_{ki} - \bar{x}_i)(y_{kj} - \bar{y}_j) \right)^2 / n^2 \sigma_i^2 \sigma_j^2 \tag{2}$$

where n is the number of runs and σ_i^2 and σ_j^2 are the variances of the input and output variables, respectively. The correlation coefficient can be interpreted as the fractional contribution to the uncertainty in the output y_j due to uncertainty in a given input parameter x_i.

Interference effects, which occur when two or more input variables act to enhance (or reduce) the uncertainty in either one by itself, can also be computed using standard statistical formulas. The calculation of interference effects can also be used to determine the importance of identifying and quantifying possible relationships (correlations) between input parameters. Correlations between input parameters that have little or no interference on the output properties of interest need not be rigorously quantified by PCA or other methodologies, as they will have little impact on the final uncertainty analysis.

The approach outline here, like all probabilistic models, requires the generation of sufficient statistics to ensure that accurate correlation coefficients are computed. Because the analysis is performed using a finite sample size (number of runs) there will always be statistical errors in the determination of the correlation coefficients. In general, sufficient runs must be performed to ensure that the magnitude of the statistical errors is small compared to the smallest uncertainties for which accurate results are desired. In practice, such analyses are typically focused on identifying the largest sources of parametric uncertainty in a given model, and thus significant errors in the predictions of the smallest uncertainty sources are acceptable. See Sec. VI.C for a discussion of the methods for ensuring numerical accuracy of the output statistics.

V. Estimation of Input Uncertainties

Even after the potentially hundreds of input parameters in a given model have been shortlisted via a preliminary sensitivity analysis, many are typically identified as requiring accurate assessments of their uncertainty. This process can be time-consuming, involving detailed literature searches and error analysis. The estimation of uncertainties associated with input parameters is often a subjective issue on which experts may express differing opinions. However, to carry out any form of probabilistic analysis, where human judgment is involved, a good practice in such instances is to consider and incorporate a variety of such expert opinions.

Statistically, uncertainty is defined as the standard error of the mean from a sample of measurements. However, because multiple measurements at relevant conditions are rarely available for the input parameters necessary for this type of analysis, the uncertainties are mostly estimated. In general, there are six ways in which the uncertainty of a given input parameter may be determined, which are as follows, in approximate order of preference:

1) Combine multiple sources of data and compute the standard error of the mean. This is the only approach that is statistically rigorous, and should be used whenever possible.

2) Perform an independent assessment of the data source. This method can be used when only a single data source is available, and requires that a detailed analysis be performed of the experimental setup, data reduction, and/or theoretical formulation.

3) Use recommendations from relevant review articles or compiled databases. In this method we rely on others to essentially perform method 1 or 2 for us. However, it is still important to ensure that the data quoted in the review article were taken at conditions relevant to the current application.

4) Use the uncertainty value quoted in the original data source. This method is commonly employed, but can be dangerous unless an independent assessment is performed to ensure that the experiment was relevant and properly performed, and that the data were reduced correctly.

5) Apply similarity rules. In this approach, the uncertainty in a given parameter is estimated from those of related parameters for which uncertainties are known via methods 1–4.

6) Rely on expert judgment. Unfortunately, this approach is used of necessity far more often than would be desired. The best way to apply this approach is to poll multiple experts on the subject and use an appropriate agglomerate value from the quoted sources.

As an example, consider the uncertainty associated with kinetic reaction rates. Uncertainties in reaction rates can be quite large, particularly at elevated temperatures typical of a hypersonic shock layer. Therefore, it is appropriate to measure such uncertainties on a logarithmic scale. The Gaussian probability distribution P of a sampled rate constant k_r can then be written as

$$P(k_r) \propto \exp\left[-\frac{1}{2} \left(\frac{\log_{10} k_r / k_r^0}{\sigma} \right)^2 \right] \tag{3}$$

where $\pm 2\sigma$ defines the 95% confidence limits that symmetrically bound the recommended rate constant k_r^0. The actual rate constant k_r thus lies within $\log_{10} k_r^0 \pm 2\sigma$ with 95% probability.

Now we consider the nitrogen dissociation reaction $N_2 + M \rightleftarrows 2N + M$, where M is a generic collision partner. This reaction is of primary importance for entries to the nitrogen-dominated atmospheres of Earth and Titan. For this reaction there are a few independent determinations of the rates for $M = N_2$ and N at flight-relevant conditions based on shock-tube data from the 1960s and 1970s. These data were examined by Park [38] using methods 1 and 2 in the context of his two-temperature (T and T_v) vibration–dissociation coupling model [39]. As shown in Fig. 1, for $M = N_2$ all

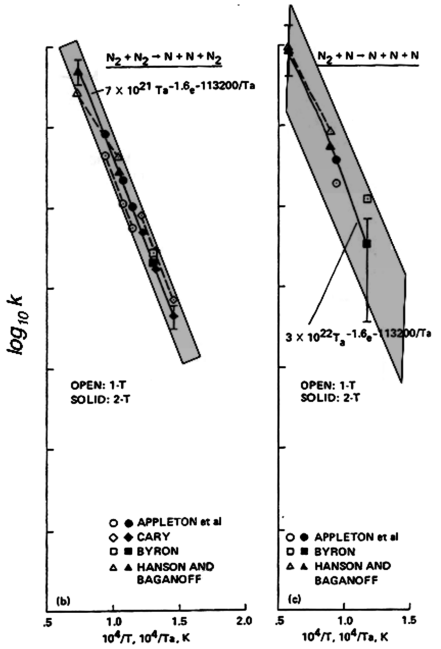

Fig. 1 Shock-tube data for N_2 dissociation rates, including estimated uncertainties (adapted from Park [38]).

available data are in good agreement within a band of about a half-order of magnitude, whereas for M = N there is considerable dispersion in the rates, particularly at low temperatures, due to a low-number density of N-atoms in the experiments at these conditions. Based on the analysis of Park [38], we assume a total uncertainty in the N_2 dissociation rate of ± 0.25 order of magnitude for $M = N_2$ and ± 0.60 order of magnitude for M = N [40]. No data are available in the literature for N_2 dissociation with other collision partners at conditions of interest for reentry; uncertainty values for other collision partners were estimated from those for N_2 and N using methods 4 and 5. Uncertainty estimates for many other reactions of interest can be taken using method 3 from the reviews of Baulch et al. [41,42], although these reviews were for combustion applications, and require significant extrapolation to conditions of interest for reentry. More recently, the online Avogadro database [43] has compiled a comprehensive list of relevant chemical processes for reentry flows, including applicable ranges and uncertainty estimates.

The preceding example highlights the varying levels of fidelity employed in the estimation of input uncertainties. To estimate the uncertainty of a single dissociation reaction with several possible collision partners four of the six possible methods were employed. Fortunately, Park [38] has already performed the complex analysis required for methods 1 and 2 for this case, but this will not always be the case. Methods of estimation for other input parameter uncertainties are discussed in more detail in [40,44]. Unfortunately, few if any quantitative data are available for many of the parameters used in modern computational aerothermodynamics and material response models, and frequently expert judgment is the only method available.

VI. Sample Results

In this section we present a sampling of results from two test cases. In each case the primary design uncertainties for the appropriate failure mode were first identified by prior analysis, which permitted the Monte Carlo analysis to focus on determining the contributions of relevant input parameters to the output uncertainty. The results summarized here are not intended to span the entire range of possible analyses, but rather to highlight the utility and power of the uncertainty analysis techniques presented in this paper. More detail on these examples can be found in the quoted references.

A. Titan Aerocapture Radiative Heating

Aerocapture at Saturn's largest moon Titan is particularly attractive, with large mass savings theoretically possible over a purely propulsive deceleration [45]. A 2002 system analysis study of this mission concept [46] selected a 4.57-m-diam, 70 deg sphere-cone geometry as the baseline for Titan aerocapture. This vehicle would enter the Titan atmosphere at approximately 6.5 km/s at an angle of attack of 16 deg. Even though this entry velocity is relatively low, preliminary aeroheating predictions [47,48] indicated that a large portion of the total heat load during the entry could come from shock-layer radiation. This radiative heating is due to the unique composition of the Titan atmosphere, which consists primarily of N_2 with a small amount ($\sim$2% by volume) of methane. This composition produces significant amounts of the CN radical behind the bow shock wave. CN radiates strongly in the violet and red bands of the spectrum, even at fairly low entry velocities. Early studies of the radiative heating environment for a Titan aerocapture mission [48,49] predicted large radiative heating rates ranging from 100–300 W/cm^2, as compared to peak laminar convective heating rates of about 50 W/cm^2. However, all of these analyses assumed that the radiative emission from the CN radical was governed by a Boltzmann distribution of the low-lying excited states. Whereas it was recognized that this model was not validated for Titan entry conditions [49], it was selected because there were no applicable ground test or flight data with which to develop a better model, and it was assumed that the Boltzmann assumption would provide a conservative estimate of the resulting radiative heat flux. The assumption of a Boltzmann distribution thus constituted a potentially large structural uncertainty for this analysis.

A preliminary parametric uncertainty analysis of Titan radiative heating was performed by Bose et al. [40] for a simplified case of an axisymmetric aeroshell to make tractable the large number of CFD runs required. Analysis was performed only at the peak heating point on the aerocapture trajectory using a 13-species chemical kinetic model [37] to account for the formation of trace species (including CN) in the Titan shock layer. A Boltzmann distribution of excited states was again assumed. A sample size (number of CFD runs) of 6000 was determined to be sufficient to provide accurate results for the 417 independent input parameters that were varied in the study. The input parameters were broken into the following categories: kinetic rates, vibration–dissociation coupling parameters, vibrational relaxation times, and transport properties (collision integrals). Details of the methodology employed to determine input uncertainties for these parameters are given in [40]. The results of the initial sensitivity study indicated that the majority of the model sensitivity was due to a small number of chemical reactions in the shock layer, as shown in Fig. 2. In fact, over 50% of the total uncertainty in the radiative heat flux was due to the interaction of N_2 and H along two possible reaction paths: $N_2 + H \rightleftarrows 2N + H$ and $N_2 + H \rightleftarrows NH + N$. These reactions were important because they impacted the vibro-electronic temperature in the shock layer, which was the controlling temperature that determined the amount of radiation from the CN molecule in the Boltzmann assumption. The uncertainty analysis indicated a mean radiative heat flux of 94 W/cm^2 with a standard deviation of 7 W/cm^2 at these conditions.

After the completion of this analysis, shock tube data were obtained in the Electric Arc Shock Tube (EAST) facility at NASA Ames and analyzed to measure radiation behind shock waves at velocities, pressures, and gas compositions compatible with the expected flight environment [50]. The results of this testing clearly indicated that the radiation measured was inconsistent with (in fact much lower than) that predicted by the Boltzmann model, as shown in Fig. 3. In the figure, distance is measured downstream of the normal shock in the tube, and the vertical line represents the end of the usable test time (data at larger distances from the shock are contaminated by impurities from the driver gas). In addition, trends anticipated from the uncertainty analysis, in particular the sensitivity of radiation intensity with freestream CH_4 mole fraction, were not observed in the experiments. These facts, together with careful analysis of the experimental data, served to indicate that the previous Boltzmann model for Titan radiative heating was in fact incorrect for the relatively low pressures encountered. As a result, a new

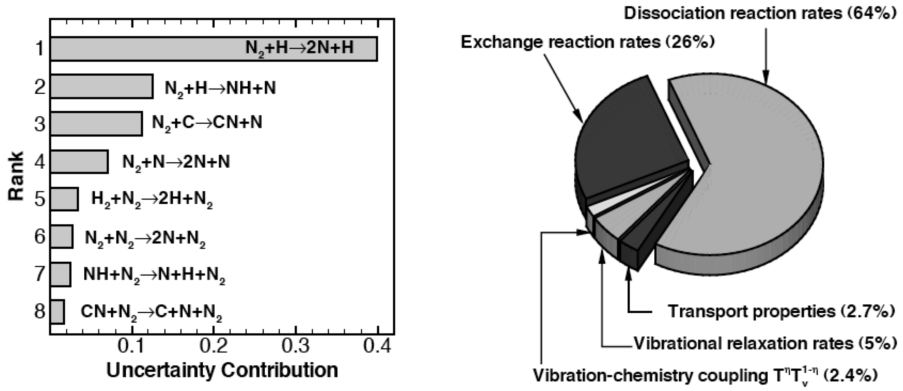

a) b)

Fig. 2 Titan radiative heating example: a) largest input uncertainty contributors, and b) contributions by category (from Bose et al. [40]).

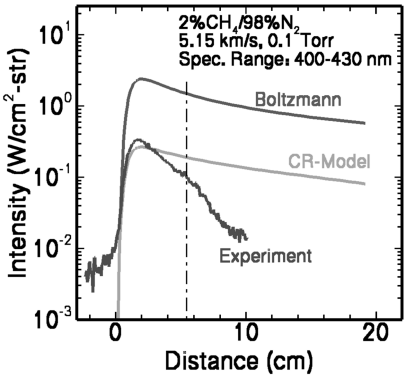

Fig. 3 Comparison of the Boltzmann and CR models to experimental data for Titan radiation (from Bose et al. [50]).

collisional-radiative (CR) model was developed and compared with the shock tube data, as shown in Fig. 3 [50].

The results of this example case serve to illustrate both the strengths of the uncertainty analysis approach, and the potential dangers if structural uncertainties in the underlying physical models are not aggressively exposed and eliminated via focused testing. The total uncertainty in Boltzmann radiative heating predicted by the parametric analysis was only $\pm 15\%$ (2σ), and was shown to be due to a small number of input parameters that would be amenable to further analysis if necessary. However, the results of the shock tube testing indicated that the Boltzmann result was too high by a factor of four. Whereas the analysis performed in [40] remains valid in terms of identifying the key input parameters that drive changes in postshock vibrational temperature, the link between vibrational temperature and radiation intensity is more complex in the collisional-radiative model than in the Boltzmann model previously employed. Clearly further testing aimed at uncertainty reduction is unwarranted until the structural uncertainty is repaired and the uncertainty analysis repeated with the corrected model.

B. Mars Pathfinder Aeroheating and TPS Sizing

Mars Pathfinder was a 2.65-m-diam, 70 deg sphere-cone, which entered the atmosphere of Mars on a ballistic (nonlifting) trajectory at a relative velocity of 7.5 km/s on 4 July 1997. Preflight calculations predicted a peak convective stagnation point heat flux of 110 W/cm^2 [51]. A postflight assessment of heat-shield temperature data concluded that the values were consistent with a peak heat flux during entry of about 85% of the predicted value [17]. As demonstrated in [44], the largest uncertainty for Mars laminar convective heating (assuming a nonablating TPS) is the catalycity of the thermal protection material. The primary catalytic reactions that are likely to occur on the vehicle surface in a dissociated CO_2 environment are

$$CO + O \rightleftarrows CO_2 \qquad \text{(R1)}$$

$$O + O \rightleftarrows O_2 \qquad \text{(R2)}$$

Although several models exist to describe surface catalycity, there are essentially no experimental data available at Mars entry conditions on relevant TPS materials with which to validate the models. As a consequence, a supercatalytic wall assumption is typically used for design. In this assumption the wall composition is forced to be equal to the freestream. This boundary condition is conservative in that the maximum chemical enthalpy is recovered at the wall, but it does not account for potential rate-limiting processes in the underlying surface chemistry (surface reaction rates are taken to be infinite). The surface catalysis model thus represents a potentially significant structural uncertainty for Mars aeroheating predictions.

A detailed uncertainty analysis of Mars Pathfinder laminar entry heating was performed by Bose et al. [44] at the peak heating point on the trajectory. The flowfield was modeled in thermochemical nonequilibrium using an eight-species kinetics model for the CO_2–N_2 atmosphere [52]. Shock-layer radiation, which was expected to contribute about 5% of the total heat load [51], was neglected. To investigate the impact of catalysis on the heating uncertainty, a parametric model was developed in [44] that allowed for the full range of catalycity to be modeled. One parameter, γ_{cat}, controls the net catalycity of the surface via both reactions R1 and R2, whereas the second parameter, p_2, controls the preference of incoming O-atoms to proceed down R2 over R1. Figure 4 shows the range of catalytic heating predictions that this model encompasses. In this manner a structural uncertainty was parametrically bounded so that it could be explored with a standard Monte Carlo analysis.

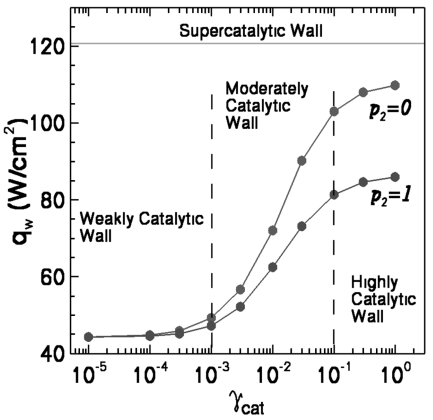

Fig. 4 Impact of catalysis modeling parameters on Pathfinder convective heating (from Bose et al. [44]).

Table 1 Uncertainty results for the stagnation point heating of Mars Pathfinder

Level of Catalycity	q_w, W/cm^2	95% confidence limits, %	
Supercatalytic	120.6	+10.3	−9.9
Highly catalytic	106.7	+12.0	−17.2
Moder. catalytic	74.0	+41.0	−33.6
Weakly catalytic	47.2	+11.7	−10.6

Inspection of Fig. 4 reveals a strong "*S*" curve in the catalytic heating as a function of γ_{cat}. As the catalycity changes, the mechanism gradually shifts from being limited by the diffusion rate of reactants to the surface (large γ_{cat}) to being limited by the rate of surface reactions (small γ_{cat}). At the low end (small γ_{cat}) of the curve the predicted heating is nearly the same for $p_2 = 0$ and $p_2 = 1$, whereas at large value of γ_{cat} much higher heating is predicted when $p_2 = 0$, which permits use of both O and CO atoms at the surface. Because the actual catalytic properties of the surface are unknown, three separate analyses were performed, for a highly, moderately, and weakly catalytic wall, to capture each portion of the "*S*" curve. In addition, a fourth analysis was performed assuming a supercatalytic wall. Each of these regions is indicated on Fig. 4.

In addition to γ_{cat} and p_2, a total of 128 other independent parameters were varied, including chemical reaction rates, vibration–dissociation coupling parameters, vibrational relaxation times, and the binary collision integrals that make up mixture transport properties. A total of 3000 DPLR runs were performed for each analysis. An assessment of the numerical accuracy of the resulting statistics as a function of the number of runs used is given in the following section. The key results of this study are summarized in Table 1. The nominal stagnation point heating rate varied from 121 W/cm^2 for a supercatalytic wall to about 47 W/cm^2 for a weakly catalytic surface, a factor of 2.5 in the predicted heat flux. More important, uncertainty estimates on the heat flux were determined in each catalytic regime. It can be seen that the supercatalytic and weakly catalytic cases have roughly symmetric uncertainty distributions of approximately $\pm 10\%$ (2σ) on predicted heating. On the other hand, the highly and moderately catalytic walls exhibit asymmetric uncertainty distributions. The largest uncertainties by far are for the moderately catalytic surface.

Figure 5 shows the key input contributors to the total uncertainty as determined via linear regression analysis. What is immediately apparent is that 1) only a small number of the 130 parameters are significant contributors to the uncertainty in heat flux, and 2) the most important parameters vary considerably for the different wall catalysis assumptions. In the pie charts all parameters that individually contribute more than 5% to the total uncertainty are labeled with the total contribution in parentheses, whereas the remainder are lumped together as "other." The binary collision integrals, which are used to compute the mixture transport properties, are denoted by the two interacting species. For the limiting case of a supercatalytic wall there is no variation in catalytic parameters, and nearly all the uncertainty comes from a small number of collision integrals that govern the rate of diffusion of the reactants CO and O to the surface. The highly catalytic wall is primarily in the diffusion limited regime, and thus the majority of the uncertainty again comes from collision integrals, although the preference factor p_2 is also important. For the moderately catalytic wall nearly all of the uncertainty comes from γ_{cat}, indicating that we are in a rate-limited regime at these conditions. Finally, for the weakly catalytic wall significant uncertainty arises from collision integrals (which in this case govern the thermal conductivity of the near wall gas), as well as a single gas-phase chemical reaction $O_2 + O \rightleftarrows 2O + O$, which affects heat release in the boundary layer.

From a design standpoint, it is clear that an improved understanding of surface catalysis for Mars entries could have a significant impact on TPS selection and design for future missions. One of the strengths of the technique presented here is that it can help to determine how much improvement is required. For example, if focused testing (or flight data) determines that a given material performs either as a highly catalytic or weakly catalytic surface, the current analysis indicates that further refinement in our knowledge of γ_{cat} may not be necessary, and additional research monies could be targeted to other risk drivers. However, if the material were determined to be moderately catalytic, the resulting heating uncertainties could be greatly reduced if the input uncertainty of γ_{cat} were reduced.

As a next step, we perform an uncertainty analysis of the stagnation point TPS material thickness for the Mars Pathfinder forebody heat shield. The forebody TPS material was Super Lightweight Ablator (SLA-561V) [53], which consists of a fiberglass–phenolic honeycomb structure filled with a charring ablative compound. The honeycomb was bonded to a graphite polyimide faceplate, which was in turn bonded to the underlying aluminum honeycomb structure. The one-dimensional TPS material

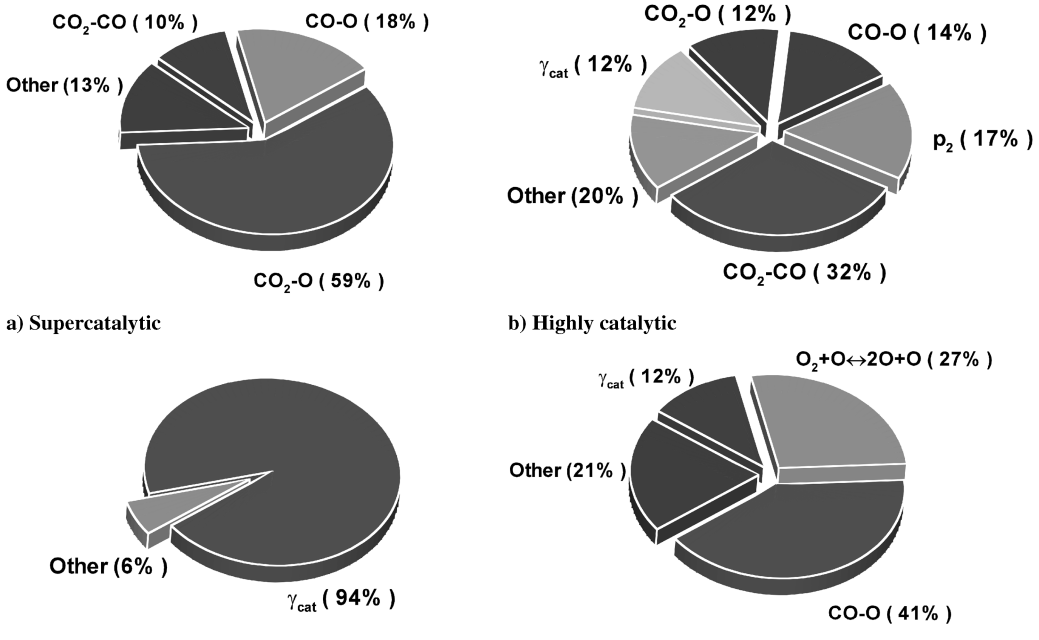

Fig. 5 Principal contributors to Pathfinder heat flux uncertainty for various wall assumptions (from Bose et al. [44]).

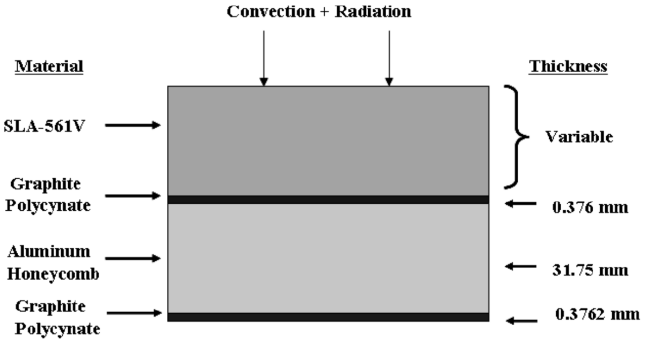

Fig. 6 Heatshield TPS material stackup for Mars Pathfinder.

stackup is shown in Fig. 6, adapted from [17]. This material has been used as a forebody TPS material on all NASA Mars entry missions to date, including Viking, Pathfinder, and MER, and on the afterbody of the Genesis and Stardust sample return capsules.

The one-dimensional ablation and thermal response simulation is performed using the fully implicit ablation thermochemistry (FIAT) code [16]. The TPS thickness is calculated based on the design maximum bond-line temperature of 250°C. The aerothermal heating history (Fig. 7a) that is used as the boundary condition of material response simulation is taken from [17], scaled slightly to match the peak supercatalytic heating predictions from [44]. The SLA-561V material response model currently used at NASA Ames considers the char formation and pyrolysis gas injection due to internal decomposition, but does not include char recession. However, at the heating rates encountered by Pathfinder the surface recession will be very small. Based on previous experience with correlating arcjet test data, thickness predictions can still be achieved with good accuracy at this heating level, even if the surface recession is ignored.

The input parameters of the sensitivity study and their estimated uncertainties in percent at a $\pm 2\sigma$ (95%) confidence level are listed in Table 2. The input parameters can be classified into three general categories: aerothermal, TPS, and substructure. The uncertainty in heat transfer coefficient is a combination of the 11% parametric uncertainty computed in [44] and an additional increment to account for stochastic uncertainties in atmospheric composition and entry state. The remaining input uncertainties are primarily determined via expert judgment, based on experience in predicting material performance during arcjet testing. A sample size of 10,000 Monte Carlo runs is performed to ensure a statistically meaningful distribution. Each run is a one-dimensional TPS sizing calculation with randomly varying input parameters. The predicted zero-margin SLA-561V thickness is 0.96 cm, and its standard deviation is 0.13 cm. The computed margined SLA thickness ($\pm 3\sigma$) is therefore 1.35 cm. Note that this applied margin accounts for aerothermal and material property variabilities, but not other sources such as atmospheric and aerodynamic dispersions, and thus is somewhat smaller than the final value that should be applied for design. The

Table 2 Uncertainties of input parameters for Mars Pathfinder TPS sizing

Category	Parameter	2σ
Aerothermal	Blowing reduction	75%
	Surface pressure	30%
	Heat transfer coefficient	25%
	Radiative heat flux	50%
TPS	Virgin density	10%
	Virgin specific heat	10%
	Virgin conductivity	20%
	Virgin emissivity	10%
	Char density	15%
	Char specific heat	20%
	Char conductivity	50%
	Char emissivity	10%
	Decomposition parameters	20%
	Pyrolysis gas enthalpy	50%
	Initial temperature	25%
Substructure	Substructure specific heat	10%
	Substructure conductivity	20%
	Substructure density	10%

normalized probability distribution function of TPS thickness is presented in Fig. 7b. In comparison, the design zero-margin thickness of SLA was 1.02 cm [53], a value in good agreement with that obtained in this work. However, a margined value of 1.52 cm was recommended for the design, and a final value of 1.91 cm was actually flown [53]. Clearly the final design of the Pathfinder heat shield was very conservative: a conclusion verified by analysis of the bondline thermocouple entry data [17]. A combination of short design cycle and a lack of a rigorous definition of uncertainties and safety margins necessitated a conservative approach.

The relative contribution of input parameters to TPS thickness is shown in the pie chart of Fig. 8. As expected, the most important uncertainty contributor to thickness is heat-shield conductivity (char and virgin), which governs the rate of conduction of heat into the TPS material and eventually into the underlying structure. Other important input uncertainties are the initial cold soak temperature and the applied convective heating rate. Heating from shock-layer radiation was not a primary uncertainty, despite its large uncertainty, because the radiative component of the total heat flux was small.

The results presented in this section for Mars Pathfinder included an assessment of both the aeroheating and TPS sizing uncertainties. However, these analyses were computed in an uncoupled manner; in other words, it was assumed that the TPS material response had no influence on the aeroheating environment encountered, and that the only influence of aeroheating on material response was through an imposed boundary condition. In reality, the environment for an ablating TPS is indeed coupled. As the material begins to char, pyrolize, and eventually ablate, carbonaceous species are injected into the boundary layer. These ablation products influence the structure of the boundary layer, affecting the convective heating rate.

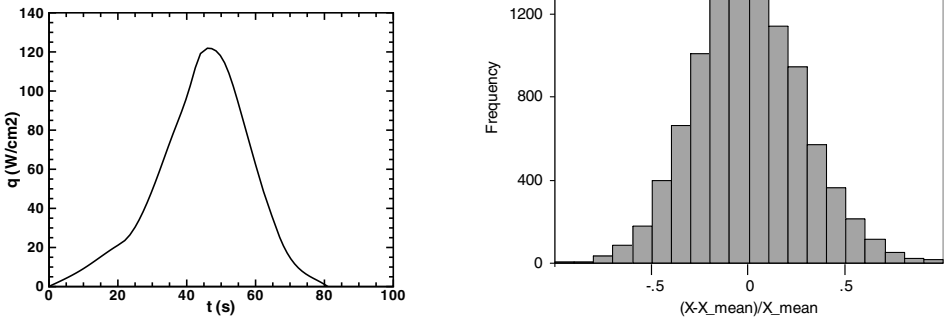

a) b)

Fig. 7 Pathfinder TPS sizing: a) aerothermal environment, and b) TPS thickness probability distribution.

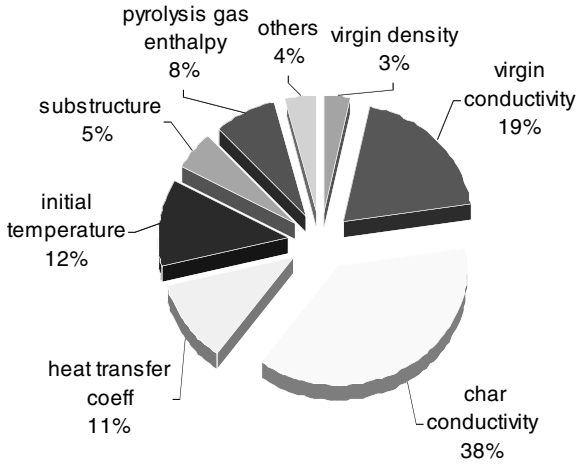

Fig. 8 Principal contributors to TPS thickness uncertainty for Mars Pathfinder.

Ablation products can also absorb or emit shock-layer radiation. Finally, as the TPS material begins to char, the catalytic properties of the surface also change, and the importance of catalytic reactions, which are now competing with oxidation, nitridation, and sublimation at the surface, are diminished [54]. A true uncertainty analysis should include the interaction between TPS material response and the aerothermal environment; this analysis has not been performed to date, but it is possible within the framework outlined in this paper.

C. Numerical Convergence Assessment

On additional piece of the puzzle is a method to ensure the numerical accuracy of the statistics that are generated by this analysis. As with any statistical methodology it is always possible to generate spurious results if the sample size is inadequate. There are three primary ways to determine the required number of runs for a given simulation. First, the distribution of input parameter uncertainties can be monitored as a function of the number of runs. If we randomly sample a Gaussian probability distribution enough times, the set of generated sample values should reproduce the required input parameter (both nominal value and uncertainty estimate).

Second, the accuracy of the resulting correlation coefficients can be estimated by sampling their confidence level as a function of the number of runs. Figure 9 shows an example of this analysis, derived from the aerothermal results for highly catalytic Mars Pathfinder simulation presented in the preceding section. In Fig. 9 the square of the correlation coefficient of five of the 130 input modeling parameters was tracked as a function of the number of runs in the Monte Carlo analysis. Three parameters (p_2, CO_2–CO, and CO–O) for which the output stagnation point heat flux is most sensitive are tracked along with two (the reaction rate for $CO_2 + O \Leftrightarrow O_2 + CO$ and the Millikan–White vibrational relaxation time for CO–O interactions) that have low sensitivity. Figure 9a plots the information on a linear scale, whereas Fig. 9b plots the same information on a log scale to highlight the results for the two parameters with low sensitivity. Also shown is the standard deviation (in percent) of the correlation coefficient over the final 500 iterations. From Fig. 9 we see that early on in the Monte Carlo process the correlations of all parameters vary wildly. However, those that have the strongest impact on the computed heat transfer converge quickly and reach asymptotic values within about 2000 Monte Carlo iterations. All of the major uncertainty contributors are converged to within a standard deviation of 2% by the time 3000 iterations are complete. Conversely, the parameters that show minimal sensitivity show larger variations (Fig. 9b), and would require more Monte Carlo iterations to converge their values. This is generally not a concern, because for most purposes it is desired to quantify only those parameters that have the strongest impact on the output, and

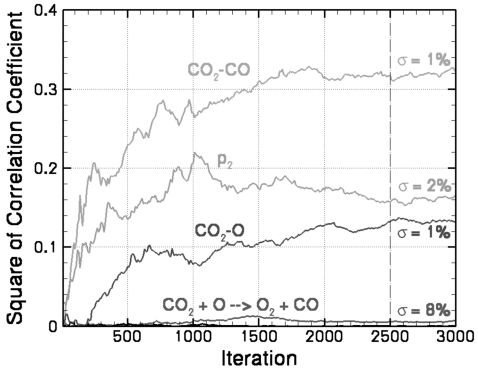

a) Linear scale

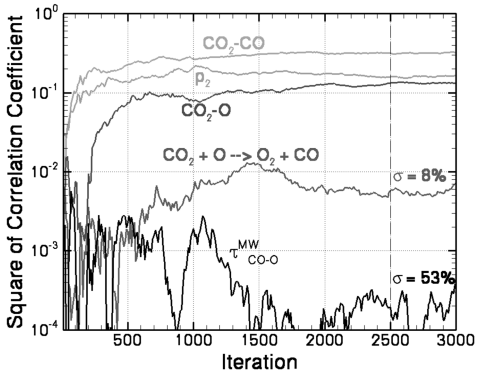

b) Log scale

Fig. 9 Sample input correlation coefficient evolution for highly catalytic Pathfinder aerothermal analysis.

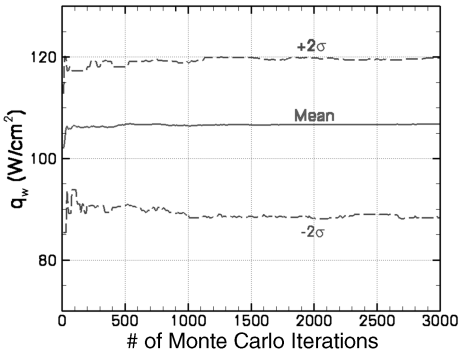

Fig. 10 Evolution of the mean and uncertainty bounds for highly catalytic Pathfinder aerothermal analysis.

large errors in the correlation coefficients for those parameters that have minimal impact is acceptable.

Finally, the mean output value and its associated uncertainty level can also be tracked as a function of the number of runs. This convergence metric is shown in Fig. 10, which plots the mean value of the stagnation point heat flux, as well as the computed 95% (2σ) confidence level as a function of the number of Monte Carlo iterations for the highly catalytic Mars Pathfinder aerothermal simulation. From the figure we see that the output heat flux and its associated uncertainty bounds converge much more rapidly than the individual sensitivities (Fig. 9). In fact, a reasonable assessment of the stagnation point aeroheating uncertainty could be made with just 500–1000 iterations in this case. Clearly the number of iterations required for a given simulation is a strong function of the desired output.

VII. Conclusions

A methodology was presented for the probabilistic sensitivity and uncertainty analysis of aerothermodynamics and thermal protection

system material response modeling for future NASA planetary exploration missions. The primary objective of this methodology is to identify and quantify the most important sources of uncertainty in aeroheating and the resulting thermal protection material selection and sizing based on inaccuracies in current knowledge of the input physical models and the modeling parameters they require. The data obtained can be used both to quantify parametric uncertainties and also to help identify structural uncertainties in the underlying models, although it is important to note that structural uncertainties cannot be identified by this approach alone. These techniques also facilitate a risk-based probabilistic design approach, whereby the TPS can be designed to a desired risk-tolerance level, and remaining risk can be effectively compared to and traded with that of other subsystems via a system-level risk mitigation analysis. Modeling sensitivities, which are a byproduct of the uncertainty analysis, can be used to rank input uncertainty drivers, which can then be prioritized and targeted for further analysis or testing. Sample results, presented for Titan aerocapture and Mars Pathfinder, demonstrate the utility of the methodology to quantify the uncertainty levels, rank sources of input uncertainty, identify structural uncertainties in the models employed, and probabilistically design a TPS for a planetary entry mission.

Acknowledgments

Funding for this work was provided by the In-Space Propulsion program under task agreement M-ISP-03-18 to NASA Ames. The authors would like to thank Peter Gage (ELORET), Dean Kontinos (NASA Ames), and Grant Palmer (ELORET) for manuscript suggestions and improvements, as well as Michelle Munk (NASA Marshall) for her unwavering support of this work.

References

[1] Johnson, L., Alexander, L., Bagett, R., Bonometti, J., Hermann, M., James, B., and Montgomery, S., "NASA's In-Space Propulsion Program: Overview and Update," AIAA Paper 2004-3841, July 2004.

[2] James, B., and Munk, M., "Aerocapture Technology Development Within the NASA In-Space Propulsion Program," AIAA Paper 2003-4654, July 2003.

[3] Thacker, B., Riha, D., Millwater, H., and Enright, M., "Errors and Uncertainties in Probabilistic Engineering Analysis," AIAA Paper 2001-1239, Jan. 2001.

[4] Garzon, V., and Darmofal, D., "Using Computational Fluid Dynamics in Probabilistic Engineering Design," AIAA Paper 2001-2526, June 2001.

[5] Gnoffo, P. A., Weilmuenster, K. J., Hamilton, H. H., Olynick, D. R., and Venkatapathy, E. V., "Computational Aerothermodynamic Design Issues for Hypersonic Vehicles," *Journal of Spacecraft and Rockets*, Vol. 36, No. 1, 1999, pp. 21–43.

[6] Anon., "Ablation Handbook, Entry Materials Data and Design," Avco Corporation, Technical Rept. AFML-TR-66-262, Mountain View, CA, Sept. 1966.

[7] Hearne, L. F., Coleman, W. D., Lefferdo, J. M., Gallagher, L. W., and Vojvodich, N. S., "A Study of the Effects of Environmental and Ablator Performance Uncertainties on Heat-Shielding Requirements for Hyperbolic Entry Vehicles," NASA CR-73224, 1968.

[8] Coleman, W. D., Hearne, L. F., Lefferdo, J. M., Gallagher, L. W., and Vojvodich, N. S., "Effects of Environmental and Ablator Performance Uncertainties on Heat-Shielding Requirements for Hyperbolic Entry Vehicles," *Journal of Spacecraft and Rockets*, Vol. 5, No. 11, 1968, pp. 1260–1270.

[9] Willcockson, W. H., "Stardust Sample Return Capsule Design Experience," *Journal of Spacecraft and Rockets*, Vol. 36, No. 3, 1999, pp. 470–474.

[10] Milos, F., Chen, Y.-K., Squire, T., and Brewer, R., "Analysis of Galileo Probe Heat Shield Ablation and Temperature Data," *Journal of Spacecraft and Rockets*, Vol. 36, No. 3, 1999, pp. 298–306.

[11] Park, C., "Laboratory Simulation of Aerothermodynamic Phenomena: A Review," AIAA Paper 92-4025, July 1992.

[12] Chen, Y.-K., Squire, T., Laub, B., and Wright, M., "Monte-Carlo Analysis for Spacecraft Thermal Protection System Design," AIAA Paper 2006-2951, June 2006.

[13] Wright, M. J., Candler, G. V., and Bose, D., "Data-Parallel Line Relaxation Method for the Navier-Stokes Equations," *AIAA Journal*, Vol. 36, No. 9, 1998, pp. 1603–1609.

[14] Cheatwood, F. M., and Gnoffo, P. A., "User's Manual for the Langley Aerothermodynamic Upwind Relaxation Algorithm (LAURA)," NASA TM 4764, April 1996.

[15] "Users Manual: Aerotherm Charring Material Thermal Response and Ablation Program," Acurex Corporation, Rept. UM-87-11/ATD, Mountain View, CA, Aug. 1987.

[16] Chen, Y.-K., and Milos, F. S., "Ablation and Thermal Analysis Program for Spacecraft Heatshield Analysis," *Journal of Spacecraft and Rockets*, Vol. 36, No. 3, 1999, pp. 475–483.

[17] Milos, F. S., Chen, Y.-K., Congdon, W. M., and Thornton, J. M., "Mars Pathfinder Entry Temperature Data, Aerothermal Heating, and Heatshield Material Response," *Journal of Spacecraft and Rockets*, Vol. 36, No. 3, 1999, pp. 380–391.

[18] Gnoffo, P., "CFD Validation Studies for Hypersonic Flow Predictions," AIAA Paper 2001-1025, Jan. 2001.

[19] Hollis, B. R., Horvath, T. J., Berry, S. A., Hamilton, H. H., and Alter, S. J., "X33 Computational Aeroheating Predictions and Comparisons with Experimental Data," AIAA Paper 99-3559, June 1999.

[20] Wright, M. J., Loomis, M. A., and Papadopoulos, P. E., "Aerothermal Analysis of the Project Fire II Afterbody Flow," *Journal of Thermophysics and Heat Transfer*, Vol. 17, No. 2, 2003, pp. 240–249.

[21] Wright, M. J., Prabhu, D. P., and Martinez, E. R., "Analysis of Apollo Command Module Afterbody Heating, Part 1: AS-202," *Journal of Thermophysics and Heat Transfer*, Vol. 20, No. 1, 2006, pp. 16–30.

[22] Desai, P. N., Mitcheltree, R. A., and Cheatwood, F. M., "Entry Dispersion Analysis for the Genesis Sample Return Capsule," *Journal of Spacecraft and Rockets*, Vol. 38, No. 3, 2001, pp. 345–350.

[23] Wilke, C. R., "A Viscosity Equation for Gas Mixtures," *Journal of Chemical Physics*, Vol. 18, No. 1, 1950, pp. 517–519.

[24] Dec, J. A., and Mitcheltree, R. A., "Probabilistic Design of Mars Sample Return Earth Entry Vehicle Thermal Protection System," AIAA Paper 2002-0910, Jan. 2002.

[25] Roache, P. J., *Verification and Validation in Computational Science and Engineering*, Hermosa, Albuquerque, NM, 1998.

[26] Roy, C., Oberkampf, W., and McWherter-Payne, M., "Verification and Validation for Laminar Hypersonic Flowfields, Part 1: Verification," *AIAA Journal*, Vol. 41, No. 10, 2003, pp. 1934–1943.

[27] Anon., "AIAA Guide for the Verification and Validation of Computational Fluid Dynamics Simulations," AIAA Paper G-077, 1998.

[28] Salari, K., and Knupp, P., "Code Verification by the Method of Manufactured Solutions," Sandia National Laboratories, Rept. No. SAND2000-1444, Albuquerque, NM, 2000.

[29] Luckring, J. M., Hemsch, M. J., and Morrison, J. H., "Uncertainty in Computational Aerodynamics," AIAA Paper 2003-0409, Jan. 2003.

[30] Roy, C., Oberkampf, W., and McWherter-Payne, M., "Verification and Validation for Laminar Hypersonic Flowfields, Part 2: Validation," *AIAA Journal*, Vol. 41, No. 10, 2003, pp. 1944–1953.

[31] Grinstead, J., Stewart, D., and Smith, C., "High Enthalpy Test Methodologies for Thermal Protection Systems Development at NASA Ames Research Center," AIAA Paper 2005-3326, May 2005.

[32] Mehta, U. B., "Guide to Credible Computer Simulations of Fluid Flows," *Journal of Propulsion and Power*, Vol. 12, No. 5, 1996, pp. 940–948.

[33] Kachigan, S. K., *Multivariate Statistical Analysis: A Conceptual Introduction*, Radius Press, New York, 1982.

[34] Saltelli, A., Chan, K., and Scott, E. M., *Sensitivity Analysis*, Wiley, New York, 2001.

[35] Park, C., "Review of Chemical-Kinetic Problems of Future NASA Missions, 1: Earth Entries," *Journal of Thermophysics and Heat Transfer*, Vol. 7, No. 3, 1993, pp. 385–398.

[36] Park, C., Howe, J. T., Jaffe, R. J., and Candler, G. V., "Review of Chemical-Kinetic Problems of Future NASA Missions, 2: Mars Entries," *Journal of Thermophysics and Heat Transfer*, Vol. 8, No. 1, 1994, pp. 9–23.

[37] Gökçen, T., "N_2-CH_4-Ar Chemical Kinetic Model for Simulations of Atmospheric Entry to Titan," AIAA Paper 2004-2469, June 2004.

[38] Park, C., "Two Temperature Interpretation of Dissociation Rate for N_2 and O_2," AIAA Paper 88-0458, Jan. 1988.

[39] Park, C., "Assessment of Two-Temperature Kinetic Model for Ionizing Air," AIAA Paper 87-1574, Jun. 1987.

[40] Bose, D., Wright, M. J., and Gökçen, T., "Uncertainty and Sensitivity Analysis of Thermochemical Modeling for Titan Atmospheric Entry," AIAA Paper 2004-2455, June 2004.

[41] Baulch, D., Cobos, C., Cox, R., Esser, C., Frank, P., Just, T., Kerr, J., Pilling, M., Troe, J., Walker, R., and Warnatz, J., "Evaluated Kinetic Data for Combustion Modeling," *Journal of Physical and Chemical Reference Data*, Vol. 21, No. 3, 1992, pp. 411–429.

[42] Baulch, D., Cobos, C., Cox, R., Frank, P., Hayman, G., Just, T., Kerr, J., Murrels, T., Pilling, M., Troe, J., Walker, R., and Warnatz, J., "Evaluated Kinetic Data for Combustion Modeling, Supplement 1," *Journal of Physical and Chemical Reference Data*, Vol. 26, No. 6, 1994, pp. 847–1033.

[43] Sergievskaya, A., "Information Support of Mathematical Modeling in Thermochemical Nonequilibrium Gases," Von Karman Lecture Series LS-2006-2, Brussels, Belgium, Feb. 2006.

[44] Bose, D., Wright, M. J., and Palmer, G. E., "Uncertainty Analysis of Laminar Aeroheating Predictions for Mars Entries," *Journal of Thermophysics and Heat Transfer*, Vol. 20, No. 4, 2006, pp. 652–662.

[45] Hall, J. L., Noca, M. A., and Bailey, R. W., "Cost-Benefit Analysis of the Aerocapture Mission Set," *Journal of Spacecraft and Rockets*, Vol. 42, No. 2, 2005, pp. 309–320.

[46] Lockwood, M. K., "Titan Aerocapture System Analysis," AIAA Paper 2003-4799, July 2003.

[47] Takashima, N., Hollis, B., Zoby, E., Sutton, K., Olejniczak, J., Wright, M., and Prabhu, D., "Preliminary Aero-thermodynamics Analysis of Titan Aerocapture Aeroshell," AIAA Paper 2003-4952, July 2003.

[48] Olejniczak, J., Wright, M., Prabhu, D., Takashima, N., Hollis, B., Zoby, E., and Sutton, K., "An Analysis of the Radiative Heating Environment for Aerocapture at Titan," AIAA Paper 2003-4953, July 2003.

[49] Wright, M. J., Bose, D., and Olejniczak, J., "The Impact of Flowfield-Radiation Coupling on Aeroheating for Titan Aerocapture," *Journal of Thermophysics and Heat Transfer*, Vol. 19, No. 1, 2005, pp. 17–27.

[50] Bose, D., Wright, M. J., Raiche, G., Bogdanoff, D., and Allen, G. A., "Modeling and Experimental Validation of CN Radiation Behind a Strong Shock Wave," *Journal of Thermophysics and Heat Transfer*, Vol. 20, No. 2, 2006, pp. 220–230.

[51] Chen, Y.-K., Henline, W. D., and Tauber, M. E., "Mars Pathfinder Trajectory Based Heating and Ablation Calculations," *Journal of Spacecraft and Rockets*, Vol. 32, No. 2, 1995, pp. 225–230.

[52] Mitcheltree, R. A., and Gnoffo, P. A., "Wake Flow About the Mars Pathfinder Entry Vehicle," *Journal of Spacecraft and Rockets*, Vol. 32, No. 5, 1995, pp. 771–776.

[53] Willcockson, W., "Mars Pathfinder Entry Heatshield Design and Flight Experience," *Journal of Spacecraft and Rockets*, Vol. 36, No. 3, 1999, pp. 374–379.

[54] Milos, F. S., and Rasky, D. J., "Review of Numerical Procedures for Computational Surface Thermochemistry," *Journal of Thermophysics and Heat Transfer*, Vol. 8, No. 1, 1994, pp. 24–34.

C. Kaplan
Associate Editor